Biochemical and Biophysical Research Communications 611 (2022) 99–106

Contents lists available at ScienceDirect

Biochemical and Biophysical Research Communications

journal homepage: www.elsevier.com/locate/ybbrc

Targeting of the glutamine transporter *SLC1A5* induces cellular senescence in clear cell renal cell carcinoma

Issei Kawakami, Hirofumi Yoshino*, Wataru Fukumoto, Motoki Tamai, Shunsuke Okamura, Yoichi Osako, Takashi Sakaguchi, Satoru Inoguchi, Ryosuke Matsushita, Yasutoshi Yamada, Shuichi Tatarano, Masayuki Nakagawa, Hideki Enokida

Department of Urology, Graduate School of Medical and Dental Sciences, Kagoshima University, Kagoshima, Japan

ARTICLE INFO

Article history:
Received 9 April 2022
Accepted 15 April 2022
Available online 20 April 2022

Keywords:
Glutamine transporter
Solute carrier family 1 member 5
V9302
Renal cell carcinoma
Cellular senescence

ABSTRACT

In recent years, cancer metabolism has attracted attention as a therapeutic target, and glutamine metabolism is considered one of the most important metabolic processes in cancer. Solute carrier family 1 member 5 (SLC1A5) is a sodium channel that functions as a glutamine transporter. In various cancer types, *SLC1A5* gene expression is enhanced, and cancer cell growth is suppressed by inhibition of SLC1A5. However, the involvement of *SLC1A5* in clear cell renal cell carcinoma (ccRCC) is unclear. Therefore, in this study, we evaluated the clinical importance of *SLC1A5* in ccRCC using The Cancer Genome Atlas database. Our findings confirmed that *SLC1A5* was a prognosis factor for poor survival in ccRCC. Furthermore, loss-of-function assays using small interfering RNAs or an SLC1A5 inhibitor (V9302) in human ccRCC cell lines (A498 and Caki1) showed that inhibition of *SLC1A5* significantly suppressed tumor growth, invasion, and migration. Additionally, inhibition of SLC1A5 by V9302 *in vivo* significantly suppressed tumor growth, and the antitumor effects of SLC1A5 inhibition were related to cellular senescence. Our findings may improve our understanding of ccRCC and the development of new treatment strategies for ccRCC.

1. Introduction

Renal cell carcinoma (RCC) accounts for 2–3% of all cancers, and the incidence of RCC increases each year. Additionally, RCC causes more than 140,000 deaths annually, representing 1% of all cancer-related deaths [1]. Despite improved treatment strategies, including tyrosine-kinase inhibitors, mammalian target of rapamycin (mTOR) inhibitors, and immune checkpoint inhibitors, to treat advanced or metastatic RCC, the therapeutic effects of these drugs are limited owing to acquired resistance. Cancer metabolism is important for cancer progression and can be targeted for cancer treatment. However, clear cell RCC (ccRCC), the most common type of RCC, has different metabolic characteristics compared with other cancers [2]. Therefore, there is a need to develop better therapeutic strategies for patients with ccRCC to target metabolic pathways.

In our previous study, we showed that the serine biosynthetic pathway was associated with resistance to hypoxia-inducible factor (HIF) 2α antagonists to avoid glycolysis dependency in advanced or metastatic ccRCC [3]. Therefore, we speculated that it may be necessary to focus on overall ccRCC metabolism to elucidate metabolic mechanisms in cancer and develop novel cancer treatments. However, measurement of metabolites using human clinical specimens is challenging owing to difficulties with sample collection and storage. Haoxin et al. identified 225 metabolites in 928 cell lines representing more than 20 cancer types in the Cancer Cell Line Encyclopedia [4], and we analyzed data from RCC cell lines to create a heat map showing the proliferative capacity of each RCC cell line when cultured with glutamine, kynurenine, asparagine, and arginine according to concentration (Fig. 1A). Interestingly, only glutamine showed concentration-dependent proliferation effects. Glutamine plays important roles in the metabolism of tumor cells, such as energy production, amino acid production, nucleotide biosynthesis. Although glutamine is a nonessential amino acid that can be synthesized from glucose, the demand for glutamine far exceeds its supply under tumorigenic conditions, and uptake of glutamine from the extracellular environment is essential [5].

* Corresponding author. Department of Urology, Graduate School of Medical and Dental Sciences, Kagoshima University, 8-35-1 Sakuragaoka, Kagoshima, 90–8520, Japan.
E-mail address: hyoshino@m3.kufm.kagoshima-u.ac.jp (H. Yoshino).

https://doi.org/10.1016/j.bbrc.2022.04.068

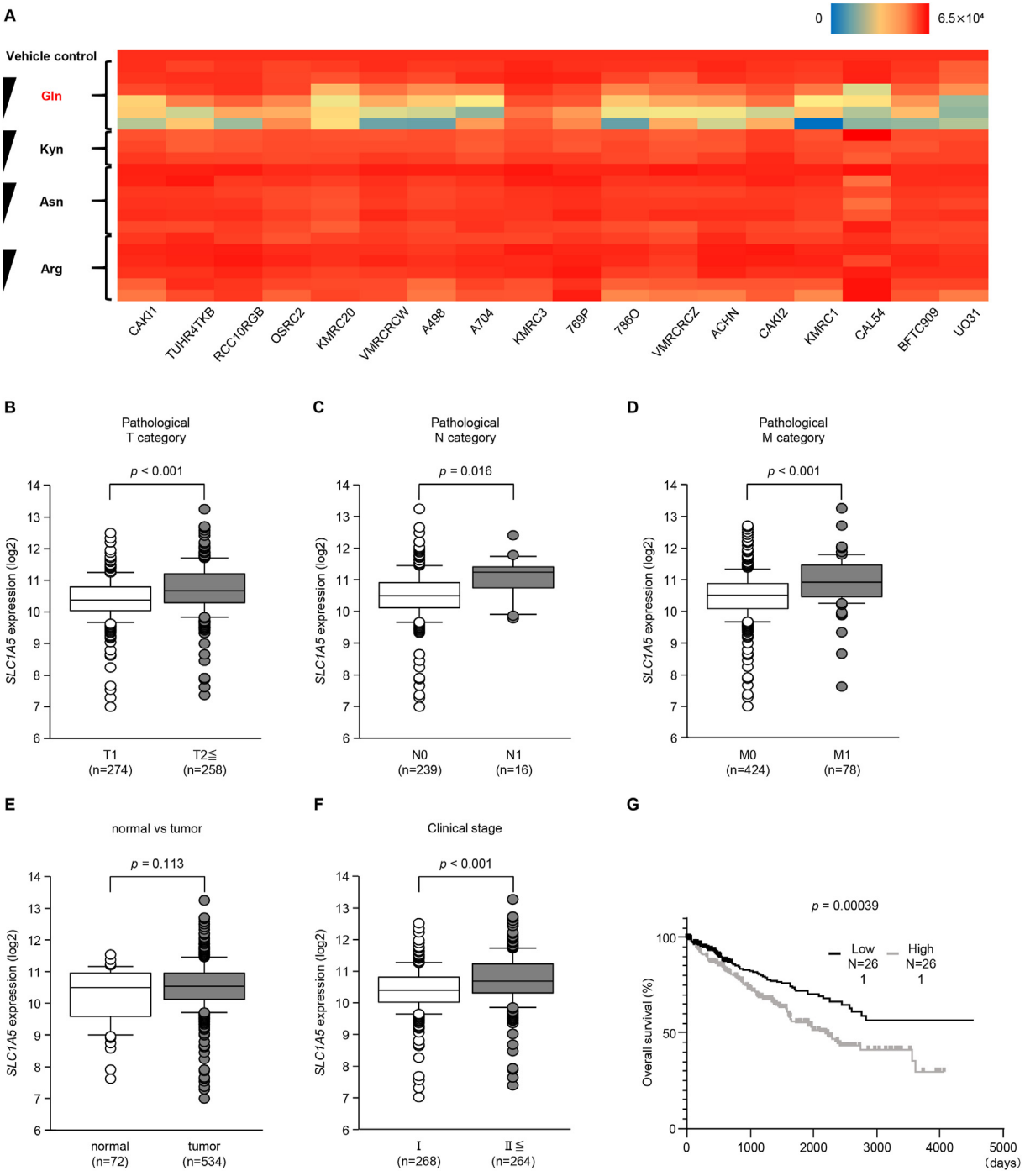

Fig. 1. (A) Heat map showing the numbers of cells for various RCC cell lines following culture with different concentrations of glutamine, kynurenine, asparagine, and arginine. (B–F) *SLC1A5* mRNA expression in RCC clinical samples. Relative *SLC1A5* mRNA expression is expressed in box plots. (G) Kaplan-Meier analysis using the OncoLnc dataset.

Accordingly, glutamine metabolism may be targeted as a novel clinical strategy for treating cancer.

Solute carrier family 1 member 5 (SLC1A5; also known as alanine, serine, cysteine transporter 2) is a neutral amino acid transporter belonging to the SLC1 family. SLC1A5 is a sodium channel that acts as a high-affinity glutamine transporter [6], and SLC1A5 expression is associated with the progression of multiple types of tumors, including colorectal cancer, gastric cancer, breast cancer, ovarian cancer, prostate cancer, and lung cancer [7–12]. In addition, Cormerais et al. identified that SLC1A5 promoted tumor growth independently of the amino acid transporter SLC1A7 (LAT1) [13]. However, the association of SLC1A5 with ccRCC progression is unclear. Additionally, novel SLC1A5 inhibitors have recently been reported [14].

Accordingly, in this study, we investigated the role of SLC1A5 in ccRCC *in vitro* and *in vivo* using an SLC1A5 inhibitor and evaluated the mechanism underlying glutamine metabolism in ccRCC.

2. Materials and methods

2.1. RCC cell lines and culture

We used human RCC cell lines A498, ACHN, Caki1, and Caki2 and HK2 that were obtained from the American Type Culture Collection (Manassas, VA, USA). Human RCC cell lines were grown in RPMI 1640 medium (Thermo Fisher Scientific, Waltham, MA, USA) supplemented with 10% fetal bovine serum (FBS; Equitech-Bio, Inc., Kerrville, TX, USA). HK2 cell line was grown in Keratinocyte Serum Free Medium (Thermo Fisher Scientific) supplemented with 0.05 mg/mL bovine pituitary extract and 5 ng/mL epidermal growth factor. These cell lines were incubated as previously described [15].

2.2. RNA extraction and RT-qPCR

To extract total RNA, cultured cells were lysed with ISOGEN (Nippon Gene, Tokyo, Japan) according to the manufacturer's protocol. The RNA concentration was measured with a spectrophotometer. To quantify *SLC1A5* expression, a SYBR green qPCR-based array approach was used as previously reported [16]. The primer sets used to measure *SLC1A5* mRNA levels were as follows: forward primer, 5′-GAGCTGCTTATCCGCTTCTTC-3′ and reverse primer, 5′-GGGGCGTACCACATGATCC-3′. Beta-glucuronidase (*GUSB*) was used as an endogenous control. The set consisted of a forward primer (5′-CGTCCCACCTAGAATCTGCT-3′) and a reverse primer (5′-TTGCTCACAAAGGTCACAGG-3′). The specificity of amplification was monitored using the dissociation curve of the amplification product. Gene expression levels compared with *GUSB* were calculated using the $2^{-\Delta\Delta CT}$ method.

2.3. Western blotting

Protein lysates were separated on NuPAGE LDS sample buffer (Thermo Fisher Scientific). The following antibodies were used for immunoblotting: anti-SLC1A5 (1:500 dilution; cat. no. 8057; Cell Signaling Technology, Danvers, MA, USA), anti-β-actin (1:5000 dilution; cat.no. bs-0061R; Bios, Beijing, China), and anti-$p21^{waf1/cip1}$ (1:500 dilution; cat. no. 2947; Cell Signaling Technology). Secondary antibodies were peroxidase-conjugated anti-rabbit IgG (1:5000 dilution; cat. no.7074S; Cell Signaling Technology) [15,17].

2.4. Small interfering RNA (siRNA) transfection

RCC cell lines were transfected with Lipofectamine RNAiMAX transfection reagent and Opti-MEM (Thermo Fisher Scientific) with 10 nM siRNA [16]. For loss-of-function experiments, *SLC1A5* siRNA (cat nos. HSS109801 and HSS109802; Thermo Fisher Scientific) and Negative Control siRNA (cat. no. D-001810-10; Dharmacon, Cambridge, UK) were used.

2.5. Cell proliferation, migration, and invasion assays

A498 and Caki1 were seeded in 96-well plates at 1000 cells/well. After 96 h, to evaluate cell proliferation, we used a XTT assays (Roche Diagnostics GmbH, Mannheim, Germany) as described previously [16]. Wound healing assays were used for cell migration activity. Cell invasion assays were performed using modified Boyden chambers consisting of Matrigel-coated Transwell membrane filter inserts with 8-μM pores in 24-well tissue culture plates (BD Biosciences, San Jose, CA, USA). The experimental procedures were performed as described in our previous study [18].

2.6. Determination of the half-maximal inhibitory concentration (IC_{50})

V-9302 was purchased from Selleck. For determination of the IC_{50} value, cells were seeded into 96-well plates at a density of 1000 cells/well in triplicate and treated with various concentrations of V-9302. After 96 h of incubation, cell proliferation was measured using XTT assays according to the manufacturer's instructions. The IC_{50} value was calculated using a nonlinear 4-parameter variable gradient equation software (GraphPad Prism, ver. 8.00; GraphPad Software, San Diego, CA, USA).

2.7. Xenograft analysis

A 100-μL suspension containing 3×10^6 A498 cells were mixed with 100 μL Matrigel matrix (Corning, Bedford, MA, USA). The suspensions were injected subcutaneously into the flanks of female nude mice (BALB/c nu/nu, 6–8 weeks old). After the tumors exceeded 100 mm^3, the mice were divided into 2 groups and treated with daily i.p. injections of vehicle (saline) or V-9302 (25 mg/kg) from day 15. All animal experiments handled in accordance with the Declaration of Helsinki, and the National Institutes of Health guide for the care and use of Laboratory animals. All animal experiments were approved by the animal care review board of Kagoshima University (approval no. MD20103).

2.8. Immunohistochemistry

Immunostaining was carried out on tissues using the UltraVision Detection System (Thermo Fisher Scientific) according to the manufacturer's protocol. Primary rabbit polyclonal antibodies against Ki-67 (cat. no. 12202; Cell Signaling Technology) were diluted 1:500. Slides were treated with biotinylated goat anti-rabbit antibodies, and diaminobenzidine hydrogen peroxidase was used as the chromogen. Counterstaining was conducted with 0.5% hematoxylin, and immunostaining was evaluated as previously described [19].

2.9. Cellular reactive oxygen species (ROS) assay

Cellular ROS assays were performed using a DCFDA/H2DCFDA-Cell ROS Assay Kit (cat. no. ab113851; Abcam, Cambridge, UK) according to the manufacturer's protocol. Briefly, human RCC cells were seeded at 1×10^5 cells/well 96-well plates, stained with DCFDA the next day, and counted using a microplate reader.

2.10. β-Galactosidase staining assay

β-Galactosidase staining assays were performed using a senescence β-galactosidase staining kit (cat. no. 9860; Cell Signaling Technology) according to the manufacturer's protocol. Briefly, cells were treated with a fixation solution (pH 6.0), and then a mixture of stains containing X-Gal was added. Cells were incubated overnight in a CO_2-free dry incubator. For quantification, six random microscopic fields of view were used, and stained cells were counted.

2.11. Statistical analysis

The relationships between two groups were analyzed using Mann-Whitney U tests. The relationships between 3 variables and numerical values were analyzed using Bonferroni-adjusted Mann-Whitney U tests. Spearman's rank tests were used to evaluate the correlation between two variables. Patients were divided into 2 or 3 groups based on the number of patients in the cohort, and differences between the two groups were evaluated by log-rank tests. All

analyses were carried out using Expert StatView software, version 5.0 (SAS Institute, Cary, NC, USA). The Cancer Genome Atlas (TCGA) cohort database of 522 patients with ccRCC was used to assess the clinical relevance of our findings. This study followed the guidelines for publication provided by TCGA. Kaplan-Meier analysis was used to analyze overall survival (OS) with data from the OncoLnc dataset (http://www.oncolnc.org).

3. Results

3.1. Clinical significance of SLC1A5 expression in ccRCC

SLC1A5 is required for glutamine uptake and is associated with various cancers. Moreover, SLC1A5 is a prognostic factor for poor survival in ccRCC. Therefore, we investigated the importance of *SLC1A5* expression in patient data from TCGA database. *SLC1A5* mRNA levels were significantly higher in patients with deep invasion, lymph node metastases, and distant metastases ($P < 0.05$; Fig. 1B–D). Although there were no significant differences in *SLC1A5* mRNA expression levels between RCC and normal samples ($P = 0.113$), the RCC samples tended to show higher expression (Fig. 1E). Moreover, *SLC1A5* mRNA expression levels were significantly higher in high-grade RCC than in low-grade RCC ($P < 0.001$; Fig. 1F). Kaplan-Meier analysis showed that patients with high *SLC1A5* mRNA expression had lower OS than patients with low *SLC1A5* expression ($P = 0.00039$; Fig. 1G). These results are consistent with previous reports showing that *SLC1A5* is a prognostic factor for poor survival in ccRCC, indicating that *SLC1A5* may also be a therapeutic target in ccRCC.

3.2. SLC1A5 knockdown suppressed ccRCC cell proliferation, migration, and invasion in vitro

Next, we examined *SLC1A5* mRNA levels in ccRCC cell lines and showed that *SLC1A5* was highly expressed in A498 and Caki1 cells (Fig. 2A). Therefore, we used these two cell lines for loss-of-function assays. We employed 2 different si-*SLC1A5* molecules that effectively downregulated SLC1A5 mRNA and protein expression in both cell lines (Fig. 2B). Suppression of *SLC1A5* significantly blocked cell proliferation, migration, and invasion (Fig. 2C–E). In invasion assays using A498 cells, *SLC1A5* knockdown blocked invasion *in vitro*.

3.3. Inhibition of SLC1A5 had antitumor effects in vitro and in vivo

Treatment of A498 and Caki1 cells with the SLC1A5 inhibitor V9302 yielded IC_{50} values of 17.7 and 24.6 μM, respectively (Fig. 3A). Cell migration and infiltration were also significantly suppressed in loss-of-function assays using V9302 (Fig. 3B and C). Next, the effects of SLC1A5 inhibition were evaluated *in vivo*. In a subcutaneous xenograft model of A498 cells, intraperitoneal administration of V9302 reduced tumor growth by more than 50% compared with control treatment (Fig. 3D). Furthermore, V9302 administration reduced body weight loss by approximately 4% compared with that in the control group (Fig. S1). Immunochemical staining showed that Ki-67 expression was significantly reduced in tumors from the V9302 group compared with those from the control group (Fig. 3E). These results suggested that inhibition of SLC1A5 by V9302 treatment resulted in antitumor effects *in vitro* and *in vivo*.

3.4. SLC1A5 inhibition increased ROS levels and induced cellular senescence

Next, we investigated the antitumor mechanisms of SLC1A5 inhibition. Glutathione, located downstream of the glutamine metabolic pathway, is known to reduce ROS, and decreased glutamine uptake owing to SLC1A5 inhibition may inhibit glutathione production, thereby increasing ROS. SLC1A5 knockdown tended to increase ROS, although the difference was not significant compared with the control (Fig. S2). Notably, elevated ROS induces cell senescence and cell cycle arrest; therefore, we hypothesized that the antitumor effects of SLC1A5 inhibition may involve these mechanisms. Staining of senescent cells with β-galactosidase was significantly enhanced by *SLC1A5* knockdown (Fig. 4A). Additionally, protein levels of the cellular senescence marker p21 were increased (Fig. 4B), and SLC1A5 inhibition by V9302 promoted cell senescence (Fig. 4C and D). Immunochemical staining of tumors resected from mice also showed a significant increase in p21 expression in the V9302 group compared with that in the control group (Fig. S3).

4. Discussion

Cancer cells reprogram metabolism for energy production and biosynthesis [20]. In particular, the Warburg effect, which preferentially uses glycolysis over oxidative phosphorylation of mitochondria for energy production even under aerobic conditions, is well known [21]. Mutations in von Hippel-Lindau are observed in more than half of ccRCC cases, resulting in increased HIF expression and suppression of mitochondrial function [22]. Thus, ccRCC is considered a metabolic disease, and targeting metabolism may lead to new therapeutic strategies for ccRCC. Indeed, in this study, we found a strong correlation between glutamine and cell proliferation in RCC cell lines [4].

Glutamine is an energy source that releases nitrogen, which is required for the production of many amino acids during conversion to glutamic acid [5]. Therefore, various glutamine-derived amino acids contribute to the survival of cancer cells. In several studies, oncogene expression is associated with increased demand for glutamine. For example, a link between oncogenic RAS and glutamine dependency has been reported in colon [23] and lung [24] cancers. When inhibiting glutamine metabolism, targeting the glutamine transporter SLC1A5 may be more effective than targeting mitochondrial glutaminase, an enzyme that converts glutamine to glutamate [14]. Moreover, blocking signaling upstream of glutamine metabolism may block multiple glutamine metabolism-related processes. Our current results indicated that *SLC1A5* was a prognostic factor for poor survival in ccRCC, consistent with previous reports [25], and that inhibition of *SLC1A5* suppressed tumor progression both *in vitro* and *in vivo*. To the best of our knowledge, this is the first report of SLC1A5 function in ccRCC.

Glutamine metabolism regulates ROS through the synthesis of glutathione, an antioxidant [5]. SLC1A5 inhibition promotes ROS generation in breast cancer [14]. However, our current results showed that *SLC1A5* knockdown tended to increase ROS, with a significant difference. Although SLC1A5 is a main transporter of glutamine, the enzyme also regulates alanine, serine, cysteine, threonine, and asparagine [6]. Therefore, inhibition of SLC1A5 may affect not only glutamine metabolism but also the metabolism of various amino acids in ccRCC. In fact, SLC1A5 inhibition by V9302 affects other metabolites, such as *N*-acetylserine, creatine phosphate, GSSG, and 4-hydroxynonenal-glutathione [14]. The involvement of glutamine in many metabolic pathways and the diverse effects of V9302 on glutamine and other metabolites may explain the discrepancies in the results for ROS levels. Notably, cancer cells require glutamine to avoid treatment-induced senescence owing to chemotherapy and radiation therapy [26]. Our results showed that inhibition of SLC1A5 promoted p21-mediated cellular senescence. Additionally, p21 expression was increased in

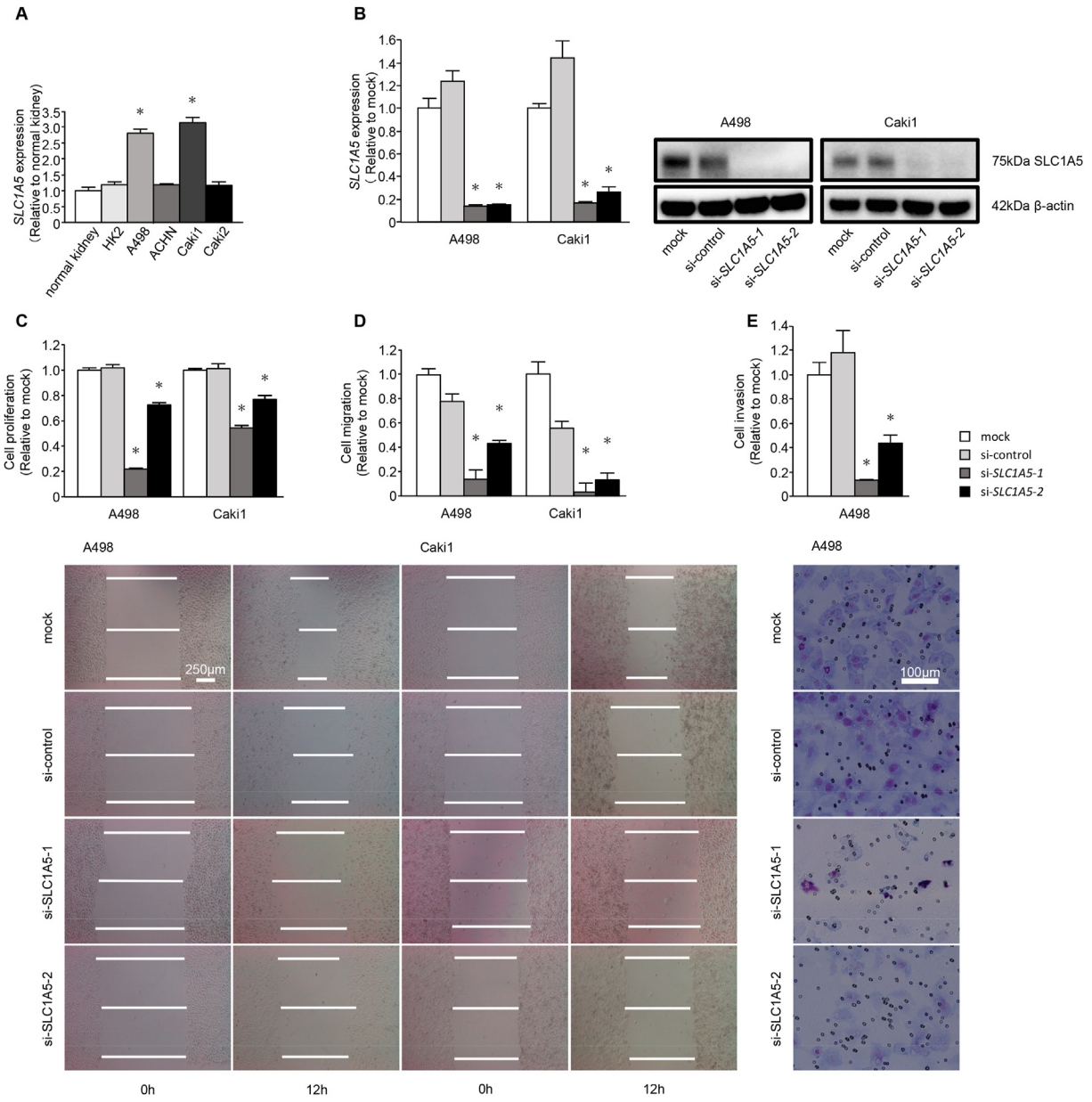

Fig. 2. Effects of *SLC1A5* knockdown in RCC cells. (A) Comparison of mRNA expression levels of *SLC1A5* in RCC cell lines by RT-qPCR (n = 3). *$P < 0.0001$. (B) The knockdown efficiency of si-*SLC1A5* was verified by evaluating *SLC1A5* mRNA expression using RT-qPCR and SLC1A5 protein levels using western blot analysis (n = 3). *$P < 0.0001$. (C) Cell proliferation was evaluated using XTT assays (n = 6). *$P < 0.0001$. (D) Cell migration activity was measured using wound healing assays (n = 3). *$P < 0.0001$. Scale bar, 250 μm. (E) Cell invasion activity was measured using Matrigel invasion assays. Invasive cells were counted and compared (n = 3). *$P < 0.01$. Scale bar, 100 μm. In all experiments, si-*SLC1A5* transfectants were compared with mock or si-control transfectants.

tumors resected from mice, although β-galactosidase staining was not definitive. Previous reports have indicated that increased ROS is also associated with cellular senescence [27] and that mTOR is essential for p53-mediated cell senescence (phosphatase and tensin homolog loss-induced cellular senescence) in other cancers [28]; however, this mechanism was not observed in the current study. Therefore, further research is needed to improve our understanding of glutamine-regulated mechanisms in ccRCC.

In this study, we administered V9302, a newly developed SLC1A5 inhibitor, in mice. However, no mice survived following daily intraperitoneal administration of 75 mg/kg V9302, consistent with a previous study [14]. Accordingly, we administered a lower dose of the inhibitor (25 mg/kg) in this study. This low dose induced sufficient antitumor effects, but also resulted in significant weight loss. Because evaluation of the IC_{50} *in vitro* showed a steep graph, V9302 may have a narrow therapeutic dose range, and side effects may occur at other concentrations; thus, the glutamine inhibitory effects of V9302 may affect both tumor and normal tissues. Further studies on changes in metabolites other than glutamine and on normal cells are needed to improve the efficacy and safety of SLC1A5-targeted treatments. Additionally, the mechanisms through which SLC1A5 inhibition exerts antitumor effects, as reported in other cancer types, e.g., apoptosis, induction of autophagy, and inactivation of mTOR signaling, need to be studied in ccRCC [14].

In summary, our study showed that high *SLC1A5* expression was associated with prognosis for poor survival in ccRCC. Furthermore, inhibition of SLC1A5 promoted cell senescence and elicited

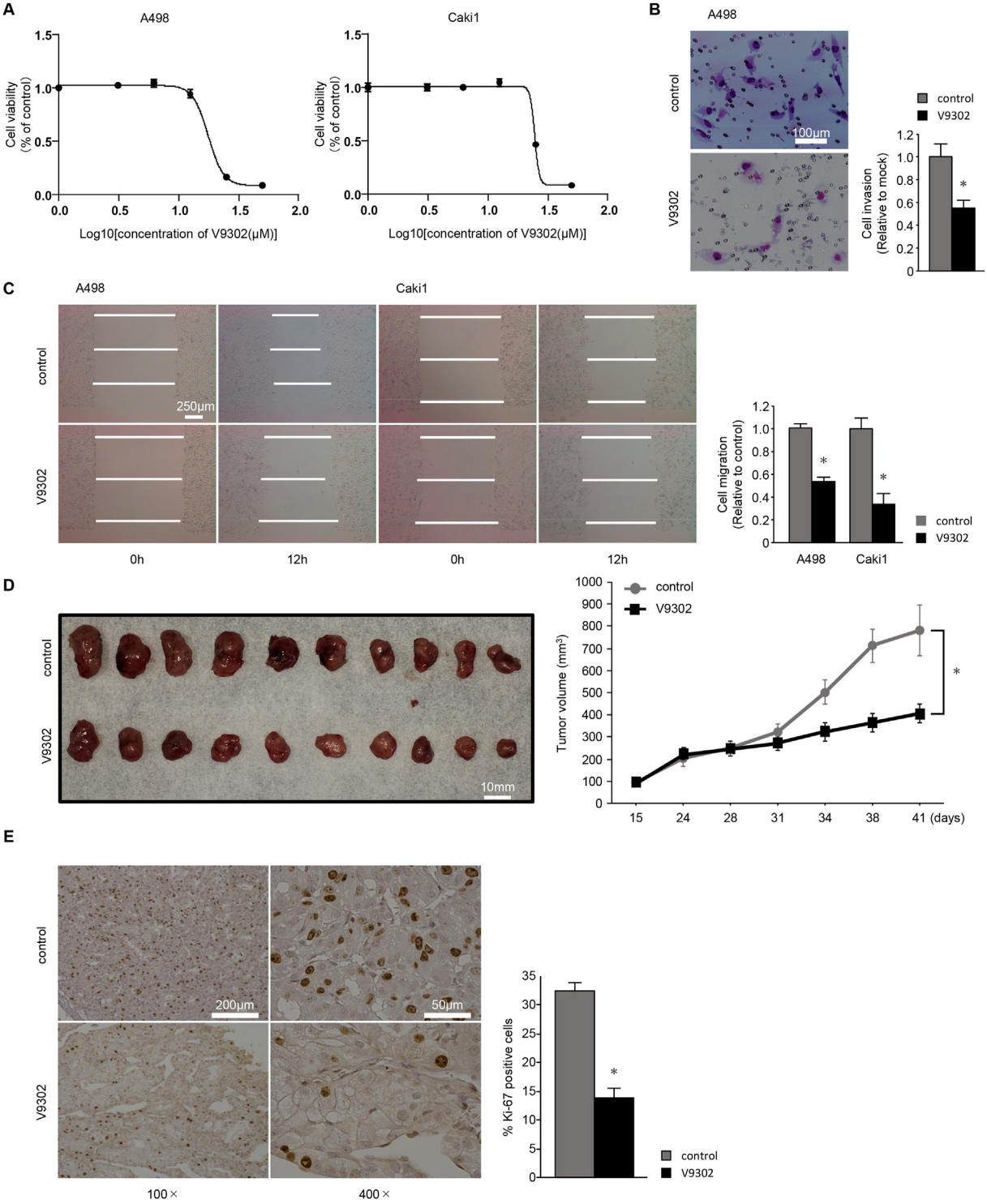

Fig. 3. Effects of V9302 *in vitro* and *in vivo*. (A) Calculated IC_{50} values for A498 and Caki1 cells (n = 6). (B) Cell invasion activity was measured using Matrigel invasion assays. Invasive cells were counted and compared (n = 3). *$P < 0.01$. Scale bar, 100 μm. (C) Cell migration activity was measured using wound healing assays (n = 3). *$P < 0.0001$. Scale bar, 250 μm. (D) Comparison of tumor volumes after intraperitoneal injection of V9302 (25 mg/kg, daily; n = 5 mice/group). *$P < 0.01$, Mann-Whitney *U* test. Photographs show resected tissues in a 41-day xenograft mouse model. (E) Comparison of tumors stained with Ki-67 after resection from mice (n = 3). *$P < 0.0001$. Scale bars, 200 μm (100 ×) and 50 μm (400 ×).

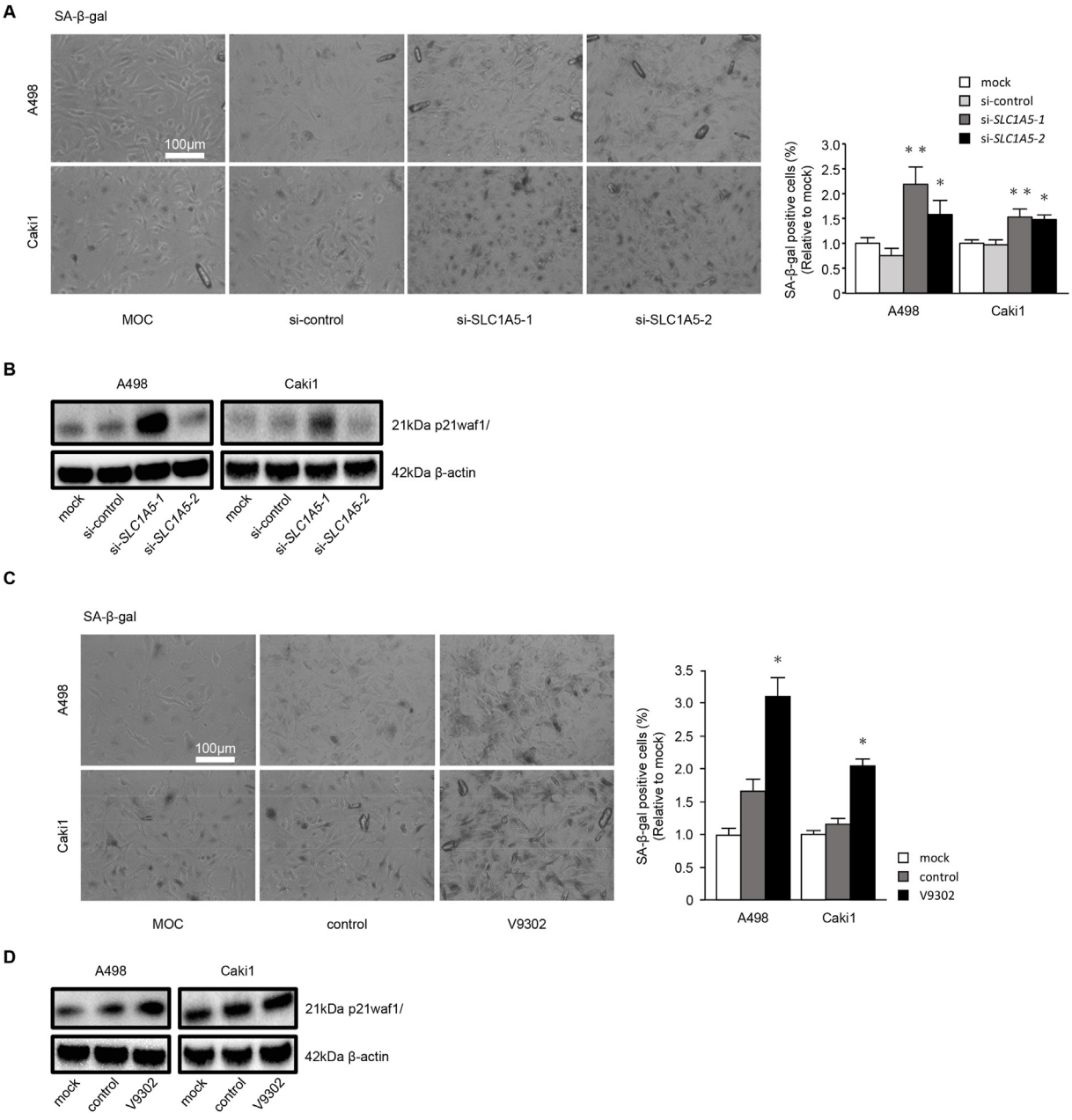

Fig. 4. Relationship between SLC1A5 and cellular senescence in RCC cells. (A) Senescence induction by si-*SLC1A5* transfection was confirmed by β-galactosidase staining (n = 6). $*P < 0.01$; $**P < 0.001$. Scale bar, 100 μm. (B) Western blot analysis of $p21^{waf1/cip1}$ expression in RCC cells transfected with si-*SLC1A5*. (C) Comparison of β-galactosidase staining between the control and V9302 groups (n = 6). $*P < 0.0001$. Scale bar, 100 μm. (D) Western blot analysis of $p21^{waf1/cip1}$ expression in RCC cells treated with V9302. Experiments were repeated at least three times. SA-β-gal, senescence-associated β-galactosidase.

antitumor effects. These results may improve our understanding of ccRCC and facilitate the development of novel treatment strategies for ccRCC.

Declaration of competing interest

None of the authors has any direct or indirect commercial financial incentives associated with the publication of this article entitled “Targeting of the glutamine transporter SLC1A5 induces cellular senescence in clear cell renal cell carcinoma”.

Acknowledgments

This research was supported by the following research funds: Japan Society for the Promotion of Science (KAKENHI; grant no. 19K09715 to Masayuki Nakagawa; grant no. 20K18146 to Yoichi Osako; grant no. 21K09404 to Hideki Enokida; grant no. 21K09430 to Yasutoshi Yamada; grant no. 19K07736 to Yoshino Hirofumi) and the Takeda Science Foundation in Japan to Hirofumi Yoshino. We are also grateful to Ms. Keiko Yoshitomi (Department of Urology, Graduate School of Medical and Dental Sciences, Kagoshima University, Kagoshima, Japan) for laboratory assistance. This work was supported by the Facility of Laboratory Animal Science Research

Support Center Institute for Research Promotion Kagoshima University. We wish to thank the Joint Research Laboratory (Kagoshima University Graduate School of Medical and Dental Sciences) for the use of their facilities.

Appendix A. Supplementary data

Supplementary data to this article can be found online at https://doi.org/10.1016/j.bbrc.2022.04.068.

References

[1] U. Capitanio, F. Montorsi, Renal cancer, Lancet 387 (2016) 894–906, https://doi.org/10.1016/s0140-6736(15)00046-x.
[2] F. Gatto, I. Nookaew, J. Nielsen, Chromosome 3p loss of heterozygosity is associated with a unique metabolic network in clear cell renal carcinoma, Proc. Natl. Acad. Sci. U.S.A. 111 (2014) E866–E875, https://doi.org/10.1073/pnas.1319196111.
[3] H. Yoshino, N. Nohata, K. Miyamoto, et al., PHGDH as a key enzyme for serine biosynthesis in HIF2alpha-targeting therapy for renal cell carcinoma, Cancer Res 77 (2017) 6321–6329, https://doi.org/10.1158/0008-5472.Can-17-1589.
[4] H. Li, S. Ning, M. Ghandi, et al., The landscape of cancer cell line metabolism, Nat. Med. 25 (2019) 850–860, https://doi.org/10.1038/s41591-019-0404-8.
[5] B.J. Altman, Z.E. Stine, C.V. Dang, From Krebs to clinic: glutamine metabolism to cancer therapy, Nat. Rev. Cancer 16 (2016) 749, https://doi.org/10.1038/nrc.2016.114.
[6] Z. Zhang, R. Liu, Y. Shuai, et al., ASCT2 (SLC1A5)-dependent glutamine uptake is involved in the progression of head and neck squamous cell carcinoma, Br. J. Cancer 122 (2020) 82–93, https://doi.org/10.1038/s41416-019-0637-9.
[7] M. Hassanein, M.D. Hoeksema, M. Shiota, et al., SLC1A5 mediates glutamine transport required for lung cancer cell growth and survival, Clin. Cancer Res. 19 (2013) 560–570, https://doi.org/10.1158/1078-0432.Ccr-12-2334.
[8] F. Huang, Y. Zhao, J. Zhao, et al., Upregulated SLC1A5 promotes cell growth and survival in colorectal cancer, Int. J Clin. Exp. Pathol. 7 (2014) 6006–6014.
[9] M. van Geldermalsen, Q. Wang, R. Nagarajah, et al., ASCT2/SLC1A5 controls glutamine uptake and tumour growth in triple-negative basal-like breast cancer, Oncogene 35 (2016) 3201–3208, https://doi.org/10.1038/onc.2015.381.
[10] K. Bjersand, T. Seidal, I. Sundström-Poromaa, et al., The clinical and prognostic correlation of HRNPM and SLC1A5 in pathogenesis and prognosis in epithelial ovarian cancer, PLoS One 12 (2017), e0179363, https://doi.org/10.1371/journal.pone.0179363.
[11] J. Lu, M. Chen, Z. Tao, et al., Effects of targeting SLC1A5 on inhibiting gastric cancer growth and tumor development in vitro and in vivo, Oncotarget 8 (2017) 76458–76467, https://doi.org/10.18632/oncotarget.19479.
[12] M.A. White, D.E. Frigo, Regulation of SLC1A4 and SLC1A5 in prostate cancer-response, Mol. Cancer Res. 16 (2018) 1811–1812, https://doi.org/10.1158/1541-7786.Mcr-18-0240.
[13] Y. Cormerais, P.A. Massard, M. Vucetic, et al., The glutamine transporter ASCT2 (SLC1A5) promotes tumor growth independently of the amino acid transporter LAT1 (SLC7A5), J. Biol. Chem. 293 (2018) 2877–2887, https://doi.org/10.1074/jbc.RA117.001342.
[14] M.L. Schulte, A. Fu, P. Zhao, et al., Pharmacological blockade of ASCT2-dependent glutamine transport leads to antitumor efficacy in preclinical models, Nat. Med. 24 (2018) 194–202, https://doi.org/10.1038/nm.4464.
[15] H. Hidaka, N. Seki, H. Yoshino, et al., Tumor suppressive microRNA-1285 regulates novel molecular targets: aberrant expression and functional significance in renal cell carcinoma, Oncotarget 3 (2012) 44–57, https://doi.org/10.18632/oncotarget.417.
[16] T. Ichimi, H. Enokida, Y. Okuno, et al., Identification of novel microRNA targets based on microRNA signatures in bladder cancer, Int. J. Cancer 125 (2009) 345–352, https://doi.org/10.1002/ijc.24390.
[17] Y. Yamada, H. Hidaka, N. Seki, et al., Tumor-suppressive microRNA-135a inhibits cancer cell proliferation by targeting the c-MYC oncogene in renal cell carcinoma, Cancer Sci 104 (2013) 304–312, https://doi.org/10.1111/cas.12072.
[18] T. Chiyomaru, H. Enokida, S. Tatarano, et al., miR-145 and miR-133a function as tumour suppressors and directly regulate FSCN1 expression in bladder cancer, Br. J. Cancer 102 (2010) 883–891, https://doi.org/10.1038/sj.bjc.6605570.
[19] H. Yoshino, T. Chiyomaru, H. Enokida, et al., The tumour-suppressive function of miR-1 and miR-133a targeting TAGLN2 in bladder cancer, Br. J. Cancer 104 (2011) 808–818, https://doi.org/10.1038/bjc.2011.23.
[20] H.I. Wettersten, O.A. Aboud, P.N. Lara Jr., et al., Metabolic reprogramming in clear cell renal cell carcinoma, Nat. Rev. Nephrol. 13 (2017) 410–419, https://doi.org/10.1038/nrneph.2017.59.
[21] M.G. Vander Heiden, L.C. Cantley, C.B. Thompson, Understanding the Warburg effect: the metabolic requirements of cell proliferation, Science 324 (2009) 1029–1033, https://doi.org/10.1126/science.1160809.
[22] A. Kinnaird, P. Dromparis, B. Saleme, et al., Metabolic modulation of clear-cell renal cell carcinoma with dichloroacetate, an inhibitor of pyruvate dehydrogenase kinase, Eur. Urol. 69 (2016) 734–744, https://doi.org/10.1016/j.eururo.2015.09.014.
[23] T. Watanabe, T. Kobunai, Y. Yamamoto, et al., Differential gene expression signatures between colorectal cancers with and without KRAS mutations: crosstalk between the KRAS pathway and other signalling pathways, Eur. J. Cancer 47 (2011) 1946–1954, https://doi.org/10.1016/j.ejca.2011.03.029.
[24] R. Romero, V.I. Sayin, S.M. Davidson, et al., Keap1 loss promotes Kras-driven lung cancer and results in dependence on glutaminolysis, Nat. Med. 23 (2017) 1362–1368, https://doi.org/10.1038/nm.4407.
[25] Y. Liu, L. Yang, H. An, et al., High expression of solute carrier family 1, member 5 (SLC1A5) is associated with poor prognosis in clear-cell renal cell carcinoma, Sci. Rep. 5 (2015) 16954, https://doi.org/10.1038/srep16954.
[26] F. Pacifico, N. Badolati, S. Mellone, et al., Glutamine promotes escape from therapy-induced senescence in tumor cells, Aging (Albany NY) 13 (2021) 20962–20991, https://doi.org/10.18632/aging.203495.
[27] A. Dimozi, E. Mavrogonatou, A. Sklirou, et al., Oxidative stress inhibits the proliferation, induces premature senescence and promotes a catabolic phenotype in human nucleus pulposus intervertebral disc cells, Eur. Cell Mater. 30 (2015) 89–102, https://doi.org/10.22203/ecm.v030a07, discussion 103.
[28] A. Alimonti, C. Nardella, Z. Chen, et al., A novel type of cellular senescence that can be enhanced in mouse models and human tumor xenografts to suppress prostate tumorigenesis, J. Clin. Invest. 120 (2010) 681–693, https://doi.org/10.1172/jci40535.